Fluctuation-induced, first-order transition in a bcc Ising model with competing interactions

M. J. Velgakis and M. Ferer
West Virginia University, Morgantown, West Virginia 26506
(Received 24 June 1982)

Landau theory predicts that the bcc, spin-$\frac{1}{2}$ Ising model with nearest-neighbor ferromagnetic interaction K_1 and next-nearest-neighbor antiferromagnetic interaction K_2 has a continuous transition with a two-component order parameter ($n=2$) between the paramagnetic and the type-II antiferromagnetic (AF_2) phases for $K_1/K_2<\frac{3}{2}$. For $K_1/K_2\lesssim\frac{3}{2}$, we show that this system has a transition temperature, determined from matching high- and low-temperature free-energy series, which is well above the temperature at which the susceptibility diverges. This supports the conclusion, also drawn from renormalization-group and Monte Carlo calculations, that the transition is driven first order by fluctuations. In the deep AF_2 regime, $K_1/K_2<1.3$, our series evidence cannot distinguish between a continuous transition and a first-order transition with small discontinuities.

I. INTRODUCTION

Transitions which Landau theory predicts to be continuous can be driven first order by the fluctuations neglected in this approximate theory.[1] We have investigated the possibility of such a fluctuation-induced first-order transition in a simple, bcc-lattice spin-$\frac{1}{2}$ Ising model with competing interactions: a nearest-neighbor (NN) ferromagnetic interaction of strength K_1 and a next-nearest-neighbor (NNN) antiferromagnetic interaction of strength K_2. The Hamiltonian of the model is

$$-\beta\mathcal{H}=K_1\sum_{\langle ij\rangle}S_iS_j-K_2\sum_{[ij]}S_iS_j\ . \tag{1.1}$$

For $K_1>1.5K_2$, the ground state of the model is one of the two ferromagnetic states with all spins aligned, $S_i=\pm1$. For $K_1<1.5K_2$, the ground state of the model is one of the four type-II antiferromagnetic (AF_2) states in which each of the two sc sublattices (A consisting of the cube corners and B of the cube centers) orders independently as a simple two sublattice antiferromagnet, i.e., $S_{A_1}=-S_{A_2}=\pm1$, where A_1 and A_2 are the two fcc sublattices of sc lattice A, similarly $S_{B_1}=-S_{B_2}=\pm1$ for the cube centers. For $K_1>1.5K_2$, Landau theory predicts a continuous transition between the paramagnetic phase and the ferromagnetic phase characterized by a one-component order parameter ($n=1$); for $K_1<1.5K_2$, Landau theory predicts a continuous transition between the paramagnetic phase and the AF_2 phase characterized by a two-component order parameter ($n=2$); and for $K_1=1.5K_2$, Landau theory predicts an $n=3$ bicritical point [Fig. 1(a)].[2-4]

Ninth-order high-temperature series for the appropriate staggered susceptibility were analyzed in the AF_2 region, $K_1<1.5K_2$.[5] The results of this analysis were inconsistent with the predictions of Landau theory in that the index γ, characterizing the divergence of the staggered susceptibility, had a value consistent with the $n=1$ universality class rather than the predicted $n=2$ universality class.[5]

An ϵ expansion predicted that noncritical modes in the Hamiltonian produced a cubic field placing the system in a region where iterations do not lead to a fixed point, which is indicative of a first-order transition.[4] Monte Carlo calculations also predicted a first-order transition in the vicinity of the expected bicritical point, $K_1\lesssim1.5K_2$.[4] Although each of these methods has its own weaknesses and ambiguities, the consistency of results from the two different methods naturally increases one's confidence in the results. Our work further strengthens this confidence because we show that the series method leads to the same results.

We have used tenth-order high-temperature susceptibility series to locate the divergence of the susceptibility determining the "second-order" phase boundary of Ref. 5. Because high-temperature (low-temperature) free-energy series should converge down (up) to the transition temperature, the temperature at which the high-temperature free energy equals the low-temperature free energy (the matching temperature) is the transition temperature in-

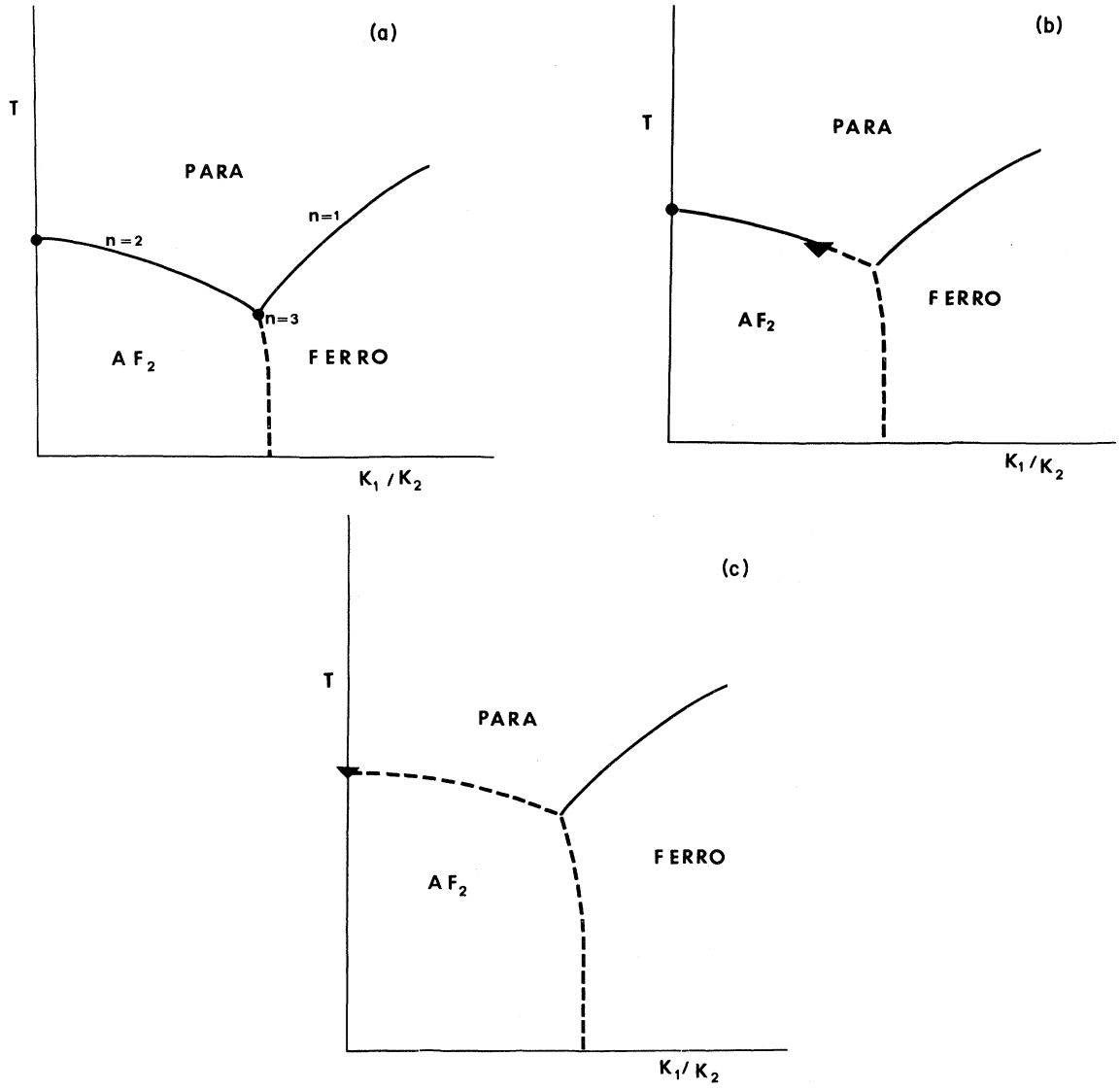

FIG. 1. Three possible choices for the phase boundary of this model. The dashed lines show first-order transitions; the solid lines show second-order transitions. ● indicates a bicritical point, while ▼ indicates a tricritical point. (a) shows the mean-field prediction. Even though our analysis favors the phase boundary in (b), it does not rule out the possibility of a first-order transition with very small discontinuities in the deep AF_2 regime, $K_1/K_2 < 1.3$, as shown in (c).

dependent of whether the transition is continuous or discontinuous.[6] Our results show that, just below the bicritical point, i.e., $K_1 \lesssim 1.5K_2$, the transition temperature is unambiguously higher than the temperature at which the susceptibility diverges. Therefore, the susceptibility does not have a divergent singularity at the transition indicative of a first-order transition; the susceptibility does have a divergent singularity at a lower temperature on a "spinodal." This is consistent with the ϵ expansion and Monte Carlo results of Ref. 4. Further into the AF_2 regime, $K_1 < 1.3K_2$, our results seem more consistent with a second-order transition; if so, the failure of the series to predict XY-like indices in this deep AF_2 regime is undoubtedly due to the failure of the short series (ten terms) to reflect the crossover from the $K_1 = 0$ Ising-type ($n = 1$) behavior to the finite K_1 XY-like ($n = 2$) behavior because the crossover is characterized by a crossover exponent which is expected to be quite small[4,7] [Figs. 1(b) and 1(c)].

In Secs. II and III we present the necessary series and discuss their derivation. In Sec. IV, we discuss

and present examples of our analysis leading to our conclusions which are discussed in Sec. V.

II. SERIES DERIVATION

In order to address the relevant questions about the order of the transitions, it is necessary to have high-temperature series for the uniform susceptibility and for the appropriate staggered susceptibility to locate the second-order phase boundary; it is also necessary to have free-energy series in the three phases to locate the phase boundary by free-energy matching. To derive the high-temperature series we have modified existing computer programs[8] for deriving tenth-order series for nearest-neighbor models so that we can derive tenth-order series for the correlation function $\langle S_{\vec{0}} S_{\vec{r}} \rangle$ of this model. The necessary high-temperature series can then be determined from these correlation function series. For the uniform susceptibility per site

$$\chi = \sum_{r_{sc}} (\langle S_{\vec{0}} S_{\vec{r}_{sc}} \rangle + \langle S_{\vec{0}} S_{\vec{r}_{sc}+\vec{b}} \rangle) = \sum_{n=0}^{\infty} a_n (K_2/K_1) K_1^n , \tag{2.1}$$

where $\vec{r}_{sc} = a(i,j,k)$ are the cube corners occupying sc sublattice A and $\vec{r}_{sc}+\vec{b}$, $\vec{b} = \frac{1}{2}a(1,1,1)$, are the cube centers occupying sublattice B. For the staggered susceptibility per site

$$\chi_s = \sum_{r_{sc}} (-1)^{i+j+k} (\langle S_{\vec{0}} S_{\vec{r}_{sc}} \rangle + \langle S_{\vec{0}} S_{\vec{r}_{sc}+\vec{b}} \rangle) = \sum_{n=0}^{\infty} b_n (K_1/K_2) K_2^n \tag{2.2}$$

associated with the AF_2 order-parameter fluctuations. For the zero-field, free-energy per site in the paramagnetic phase

$$-\beta F = \ln 2 - \int_0^{\beta} E(\beta') d\beta' = \ln 2 + \sum_{n=2}^{\infty} f_{P,n} (K_2/K_1) K_1^n , \tag{2.3}$$

where $E(\beta)$ is the energy per site given by

$$E(\beta) = -4J_1 \langle S_{\vec{0}} S_{(a/2)(1,1,1)} \rangle + 3J_2 \langle S_{\vec{0}} S_{a(1,0,0)} \rangle , \tag{2.4}$$

where $K_\alpha = \beta J_\alpha$. The new series for χ, χ_s, and $-\beta F$ are given in Tables I, II, and III, respectively.

TABLE I. Coefficients in the high-temperature susceptibility series (2.1).

n	$a_n(x = K_2/K_1)$
0	1
1	$8 - 6x$
2	$56 - 96x + 30x^2$
3	$389\frac{1}{3} - 984x + 768x^2 - 148x^3$
4	$2610\frac{2}{3} - 8992x + 10\,704x^2 - 5248x^3 + 706x^4$
5	$17\,473\frac{1}{15} - 74\,800x + 12\,3104x^2 - 93\,488x^3 + 32\,704x^4 - 3360.8x^5$
6	$115\,250\frac{22}{45} - 597\,324.8x + 1\,234\,120x^2 - 1305\,898\frac{2}{3}x^3 + 716\,944x^4 - 192\,588.8x^5 + 15\,753\frac{1}{3}x^6$
7	$759\,545\frac{221}{315} - 4\,579\,739\frac{11}{15}x + 11\,520\,102.4x^2 - 15\,406\,570\frac{2}{3}x^3 + 11\,854\,730\frac{2}{3}x^4 - 504\,3011.2x^5 + 1088\,802\frac{2}{15}x^6 - 7\,375\,367\frac{13}{21}x^7$
8	$4\,966\,694\frac{26}{45} - 34\,386\,356\frac{44}{105}x + 101\,103\,355\frac{11}{15}x^2 - 165\,271\,099\frac{11}{15}x^3 + 161\,551\,909\frac{1}{3}x^4 - 96\,768\,302\frac{14}{15}x^5 + 33\,341\,947\frac{11}{15}x^6 - 5\,977\,370\frac{86}{105}x^7 + 342\,619\frac{31}{105}x^8$
9	$32\,458\,605.211\,992 - 252\,399\,713.523\,79x + 854\,687\,254.552\,37x^2 - 1\,638\,855\,259.0223x^3 + 1\,964\,204\,200.5332x^4 - 1\,500\,892\,997.3331x^5 + 730\,987\,764.622\,33x^6 - 210\,393\,177.295\,29x^7 + 32\,069\,724.038\,057x^8 - 1\,590\,370.289\,9469x^9$
10	$211\,100\,973.265\,04 - 1\,829\,175\,811.1151x + 6\,975\,616\,824.3807x^2 - 15\,440\,906\,690.642x^3 + 21\,770\,155\,032.178x^4 - 20\,449\,276\,648.104x^5 + 12\,749\,667\,633.777x^6 - 5\,204\,224\,779.7855x^7 + 1\,280\,085\,077.1811x^8 - 169\,006\,631.686\,42x^9 + 7\,346\,967.445\,501\,3x^{10}$

TABLE II. High-temperature staggered susceptibility series (2.2).

n	$b_n(y=K_1/K_2)$
0	1
1	6
2	$30-8y^2$
3	$148-24y^2$
4	$706-336y^2-34\frac{2}{3}y^4$
5	$3360.8-1072y^2+688y^4$
6	$15\,753\frac{1}{3}-10\,672y^2-4792y^4-869\frac{31}{45}y^6$
7	$73\,753\frac{71}{105}-35\,139.2y^2+55\,338\frac{2}{3}y^4+20\,238\frac{14}{15}y^6$
8	$342\,619\frac{31}{105}-297\,646\frac{14}{15}y^2-308\,357\frac{1}{3}y^4-306\,542\frac{14}{15}y^6-20\,710\frac{134}{315}y^8$
9	$1\,590\,370\frac{274}{945}-1\,010\,278\frac{74}{105}y^2+2\,789\,291\frac{11}{15}y^4+3\,497\,051\frac{1}{45}y^6$ $+715\,387\frac{117}{945}y^8$
10	$7\,346\,967\frac{421}{945}-7\,749\,409\frac{1}{15}y^2-14\,348\,047\frac{29}{45}y^4-35\,265\,466\frac{14}{45}y^6$ $-14\,263\,537\frac{1}{15}y^8-557\,079\frac{58}{105}y^{10}$

In the ferromagnetic phase, seventh-order high-field series were derived in Ref. 9. In the limit of zero field, these series can be recast as a low-temperature series through eighteenth order in the variable $u_D=e^{-2K_2-(4K_1-6K_2)}$ (the ferromagnetic regime occurs for $4K_1>6K_2$)

$$-\beta F=(4K_1-3K_2)+\tfrac{1}{4}\sum_{n=0}^{\infty} f_n(z)u_D^n\,, \qquad (2.5)$$

where $z=e^{-2K_2}$. These series for the free energy per site are presented in Table IV.

III. DERIVATION OF THE LOW-TEMPERATURE AF_2 SERIES

We start from one of the four equivalent AF_2 ground states, specifically $S^{A_1}=S^{B_1}=-S^{A_2}=-S^{B_2}=1$, and perform a standard cluster expansion in the number of overturned spins.[10] Since this expansion is usually derived as a strong field expansion, we modify the Hamiltonian in (1.1) by adding not only a uniform field h but also a staggered field

TABLE III. High-temperature free energy series (2.3).

n	$f_{P,n}(x=K_2/K_1)$
2	$2+1.5x^2$
3	$-12x$
4	$11\frac{2}{3}+48x^2+2.75x^4$
5	$-160x-200x^3$
6	$132\frac{4}{45}+1438x^2+820x^4+18\frac{1}{15}x^6$
7	$-3176\frac{8}{15}x-10\,810\frac{2}{3}x^3-3505.6x^5$
8	$2214\frac{47}{126}+45\,578\frac{2}{15}x^2+73\,557\frac{1}{3}x^4+14\,794\frac{2}{15}x^6+147\frac{67}{840}x^8$
9	$-77\,263\frac{5}{21}x-50\,677\frac{5}{9}x^3-467\,381\frac{1}{3}x^5-63\,820\frac{20}{21}x^7$
10	$45\,866\frac{622}{2025}+1\,527\,410\frac{58}{105}x^2+4\,811\,148\frac{4}{9}x^4+2\,830\,714\frac{26}{45}x^6$ $+273\,568\frac{100}{105}x^8+1531\frac{8238}{14175}x^{10}$
11	$-2\,098\,511.214\,389\,4x-22\,491\,733.434\,917x^3-40\,972\,237.937\,782x^5$ $-16\,530\,630.298\,401x^7-1\,190\,001.278\,309\,5x^9$

TABLE IV. Low-temperature free-energy series in the ferromagnetic phase (2.5).

n	$f_n(z=e^{-2K_2})$
4	$4z^2$
7	$16z^2$
8	$-30z^4+12z^6$
10	$64z^2+48z^4$
11	$-352z^4+96z^6$
12	$24z^2+24z^4+373\frac{1}{3}z^6-288z^8+60z^{10}$
13	$288z^2+384z^4+144z^6$
14	$-2808z^4-720z^6+384z^8$
15	$192z^2+480z^4+7872z^6-4608z^8+720z^{10}$
16	$1416z^2+1968z^4+1188z^6-4203z^8+6564z^{10}-2586z^{12}+332z^{14}+12z^{16}$
17	$144z^2-20160z^4-15384z^6+1440z^{10}$
18	$16+1392z^2+4368z^4+99360z^6-14400z^8-13680z^{10}+2976z^{12}+96z^{14}$

h_s coupled to the chosen ordered state

$$-\beta\mathcal{H}=K_1\sum_{\langle ij\rangle}S_iS_j-K_2\sum_{[ij]}S_iS_j+h\sum_i S_i+h_s\sum_i g_iS_i\ , \tag{3.1}$$

where $g_i=+1$ on A_1 and B_1 sites and -1 on A_2 and B_2 sites. The lattice gas reformulation of this Hamiltonian

$$\begin{aligned}-\beta\mathcal{H}=&(3K_2+h_s)N\\&+4K_1\sum_{\langle ij\rangle}(n_i^{A_1}-n_i^{A_2})(n_j^{B_1}-n_j^{B_2})\\&+4K_2\sum_{[ij]}(n_i^{A_1}n_j^{A_2}+n_i^{B_1}n_j^{B_2})\\&+\sum_i\sum_{\alpha=A}^{B}\sum_{l=1}^{2}\beta\mu^{\alpha_l}n_i^{\alpha_l}\end{aligned} \tag{3.2a}$$

with the occupation numbers

$$\begin{aligned}&n_i^{A_1}=\tfrac{1}{2}(1-S_i^{A_1})\ ,\quad n_i^{A_2}=\tfrac{1}{2}(1+S_i^{A_2})\ ,\\&n_i^{B_1}=\tfrac{1}{2}(1-S_i^{B_1})\ ,\quad n_i^{B_2}=\tfrac{1}{2}(1+S_i^{B_2})\ ,\end{aligned} \tag{3.2b}$$

chosen so that the magnetic ground state is the vacuum state ($n_i=0$) of the lattice gas. The chemical potentials used in the Hamiltonian are given by

$$\begin{aligned}&\beta\mu^{A_1}=\beta\mu^{B_1}=-12K_2-2h-2h_s\ ,\\&\beta\mu^{A_2}=\beta\mu^{B_2}=-12K_2+2h-2h_s\ .\end{aligned} \tag{3.2c}$$

Note that in going from (3.1) to (3.2a)—(3.2c), we have changed from a notation where i labels one of N sites on the bcc lattice to a notation where i labels one of the $N/4$ primitive cells (which form an fcc lattice) containing 4 sites—one A_1 site, one B_1 site, etc.

Performing a cluster expansion in the number of "particles" (overturned spins) for this Hamiltonian gives a free energy of the form

$$\begin{aligned}-N\beta F=&+\ln\mathrm{Tr}\,e^{-\beta\mathcal{H}}\\&=(3K_2+h_s)N+\sum[\alpha,\beta,\gamma,\delta,r,s]\\&\qquad\times X_1^{\alpha+\gamma}X_2^{\beta+\delta}b_1^rb_2^s\ ,\end{aligned} \tag{3.3}$$

where $X_m=e^{\beta\mu_{Am}}=e^{\beta\mu_{Bm}}$, $b_1=e^{-4K_1}$, $b_2=e^{+4K_2}$, and where the coefficient $[\alpha,\beta,\gamma,\delta,r,s]$ gives the free-energy contribution from α overturned A_1 spins, β overturned A_2 spins, γ overturned B_1 spins, and δ overturned B_2 spins with r nearest-neighbor (NN) pairs and s next-nearest-neighbor (NNN) pairs. In actually deriving the cluster expansion we have used a modification of the shadow lattice method of Sykes *et al.*[9] in which we determined the partial generating functions

$$NF_{\alpha\beta\gamma}=\sum_{\delta=0}^{\infty}\sum_{r,s}[\alpha,\beta,\gamma,\delta,r,s]X_2^{\delta}b_1^rb_2^s$$

by simple combinatorics for a configuration of α A_1 sites, β A_2 sites, and γ B_1 sites, and from these the free-energy coefficients. For example, if you have one occupied A_1 site with all A_2 and B_1 sites empty $(\alpha,\beta,\gamma)=(1,0,0)$, there are $N/4$ ways of occupying one of the A_1 sites. If you then put r particles on the four B_2 sites which are nearest neighbors to the

occupied A_1 site and t particles on any of the other $(\frac{1}{4}N-4)$ B_2 sites, the contribution to the partition function is the number of ways of putting r particles on the four NN sites times the number of ways of putting t particles on the remaining $(\frac{1}{4}N-4)$ sites times the energy weight factor, i.e.,

$$\frac{N}{4}X_1\begin{bmatrix}4\\r\end{bmatrix}\begin{bmatrix}\frac{N}{4}-4\\t\end{bmatrix}b_1^r X_2^{r+t}\,, \tag{3.4}$$

where

$$\begin{bmatrix}4\\r\end{bmatrix}$$

is the binomial coefficient

$$\frac{4!}{r!(4-r)!}\,.$$

Note, given our Hamiltonian the particles on the B_2 sites interact only with particles on other sublattices not with each other. The contribution to the free energy is the part of the contribution to the partition function which is linear in N, i.e.,

$$\frac{N}{4}X_1\begin{bmatrix}4\\r\end{bmatrix}\begin{bmatrix}-4\\t\end{bmatrix}b_1^r X_2^{r+2}$$

so that the contribution to the free energy for one occupied A_1 site and all numbers of particles on the B_2 sites is

$$X_1F_{100}=\tfrac{1}{4}X_1\sum_{r=0}^{4}\sum_{t=0}^{\infty}\begin{bmatrix}+4\\r\end{bmatrix}\begin{bmatrix}-4\\t\end{bmatrix}(b_1X_2)^rX_2^t$$

$$=\tfrac{1}{4}X_1(1+b_1X_2)^4/(1+X_2)^4\,. \tag{3.5}$$

The partial generating functions for other values of (α,β,γ) can be found in a similar way. The main advantages of this method are that one only need consider the number of ways of putting particles on three of the sublattices and that sublattice symmetries provide relations between the free energy coefficients

$$\begin{aligned}&[\alpha,\beta,\gamma,\delta,r,s]=[\beta,\alpha,\gamma,\delta,-r,s]\,,\\&[\alpha,\beta,\gamma,\delta,r,s]=[\alpha,\beta,\delta,\gamma,-r,s]\,,\\&[\alpha,\beta,\gamma,\delta,r,s]=[\gamma,\delta,\alpha,\beta,r,s]\,,\end{aligned} \tag{3.6}$$

which enable one to determine unknown coefficients from ones already derived: e.g., the coefficient for $[\alpha,\beta,\gamma,\delta]=[1,0,0,4]$ can be determined from the partial generating function in (3.5); from [1,0,0,4] and the relations in (3.6) one can then determine the coefficients [1,0,4,0], [4,0,1,0], [4,0,0,1], [0,4,0,1], [0,4,1,0], [0,1,0,4], and [0,1,4,0], which significantly reduces the amount of actual labor which is to be performed.

The partial generating functions necessary to derive fifth-order high-staggered-field series are tabulated in Table V. In the limit of zero-uniform field, the high-staggered-field series takes the form

$$\begin{aligned}-\beta NF&=N(3K_2+h_s)+\sum_{\alpha\beta\gamma\delta}\sum_r\sum_s[\alpha,\beta,\gamma,\delta,r,s]X^{\alpha+\beta+\gamma+\delta}b_1^rb_2^s\\&=N(3K_2+h_s)+N\sum_{n=1}^{\infty}L_n(u_1,u_2)\mu^n\,,\end{aligned} \tag{3.7a}$$

where

$$NL_n(u_1,u_2)=\sum_{\substack{\alpha\beta\gamma\delta\\ n=\alpha+\beta+\gamma+\delta}}\sum_r\sum_s[\alpha,\beta,\gamma,\delta,r,s]u_1^ru_2^{3n-s} \tag{3.7b}$$

and where $u_1=b_1$, $u_2=b_2^{-1}$, $\mu=e^{-2h_s}$, and $X=\mu u_2^3$.

The polynomials $L_n(u_1,u_2)$ for $n\leq 5$ are given in Table VI. Since we are interested in the free energy with zero-applied field, we must also take the limit of zero-staggered field. In this limit, the natural expansion variable is the low-temperature variable $u_2=e^{-4K_2}$. To determine the correct coefficients in this low-temperature series we need to know how undetermined L_n's contribute. For example, we are able to determine the coefficients in the low-temperature series through twelfth order in u_2 for the following reasons. Earlier work on the nearest-neighbor Ising model for the simple-cubic lattice, to which our model reduces if $K_1=0$, shows that there are contributions of order u_2^{11} and u_2^{12} to L_6 from six-point cluster diagrams with seven and six u_2^{-1} lines (NNN bonds) respectively, and that there are contributions of order u_2^{12} to L_7 from seven-point

TABLE V. Partial generating functions. In this table we have used a modification of the code in Sykes *et al.* (Ref. 10) where, e.g., $(k,mb_1,nb_1^{-1},pb_1b_2,qb_2,rb_2^2)=(1+b_1X)^m(1+b_1^{-1}X)^n(1+b_1b_2X)^p(1+b_2X)^q(1+b_2^2X)^r/(1+X)^k$.

$$2F_{000}=\tfrac{1}{2}\ln(1+X)$$
$$2F_{100}=\tfrac{1}{2}(4,4b_1)$$
$$2F_{001}=\tfrac{1}{2}(6,6b_2)$$
$$2F_{200}=3(7,b_1^2,6b_1)-3\tfrac{1}{4}(8,8b_1)$$
$$2F_{002}=3(10,2b_2^2,8b_2)+\tfrac{3}{2}(11,b_2^2,10b_2)-4\tfrac{3}{4}(12,12b_2)$$
$$2F_{110}=3b_2(4,2b_1,2b_1^{-1})+2(6,3b_1,3b_1^{-1})-5(8,4b_1,4b_1^{-1})$$
$$2F_{101}=2b_1^{-1}(7,b_1,3b_1b_2,3b_2)+6(9,3b_1,b_1b_2,5b_2)-8(10,4b_1,6b_2)$$
$$\begin{aligned}2F_{003}=&4(13,b_2^3,3b_2^2,9b_2)+6(14,b_2^3,2b_2^2,11b_2)+15(14,4b_2^2,10b_2)+24(15,3b_2^2,12b_2)\\&+7\tfrac{1}{2}(16,2b_2^2,14b_2)-84(16,2b_2^2,14b_2)-48(17,b_2^2,16b_2)+75\tfrac{2}{3}(18,18b_2)\end{aligned}$$
$$\begin{aligned}2F_{300}=&2(9,3b_1^2,6b_1)+21(10,2b_1^2,8b_1)-60(11,b_1^2,10b_1)\\&+2(10,b_1^3,9b_1)+35\tfrac{1}{6}(12,12b_1)\end{aligned}$$
$$\begin{aligned}2F_{210}=&6b_2^2(6,5b_1,b_1^{-1})+6b_2(8,6b_1,2b_1^{-1})+\tfrac{3}{2}b_2^2(4,4b_1)+3(8,6b_1,2b_1^{-1})\\&+18b_2(7,b_1^2,4b_1,2b_1^{-1})-48(11,b_1^2,6b_1,4b_1^{-1})-38(10,7b_1,3b_1^{-1})\\&-48b_2(8,6b_1,2b_1^{-1})+18(9,b_1^2,5b_1,3b_1^{-1})+6b_2(6,5b_1,b_1^{-1})+75\tfrac{1}{2}(12,8b_1,4b_1^{-1})\end{aligned}$$
$$\begin{aligned}2F_{102}=&3b_1^{-2}(10,2b_1b_2^2,2b_1b_2,6b_2)+3(12,2b_1,2b_1b_2,6b_2,2b_2^2)+6b_1^{-1}(12,b_1,2b_1b_2,b_1b_2^2,8b_2)\\&+24(14,2b_1,2b_1b_2,10b_2)+12b_1^{-1}(11,b_1,2b_1b_2,2b_1b_2^2,b_2^2,6b_2)+42(13,3b_1,b_1b_2,2b_2^2,7b_2)\\&+6b_1^{-1}(11,b_1,3b_1b_2,2b_2^2,5b_2)+6b_1^{-1}(12,4b_1b_2,8b_2)+30(14,3b_1,b_1b_2,b_2^2,9b_2)\\&+6b_1^{-1}(12,b_1,3b_1b_2,b_2^2,7b_2)-44b_1^{-1}(13,b_1,3b_1b_2,9b_2)-42(15,4b_1,b_2^2,10b_2)\\&-168(15,3b_1,b_1b_2,11b_2)-72(14,4b_1,2b_2^2,8b_2)+182(16,4b_1,12b_2)+6(13,3b_1,b_1b_2^2,b_2^2,8b_2)\end{aligned}$$
$$\begin{aligned}2F_{111}=&6b_1b_2(8,2b_1,2b_1^{-1}b_2,4b_2)+6b_1^{-1}b_2(8,2b_1^{-1},2b_1b_2,4b_2)+6b_2(8,b_1,b_1^{-1},b_1b_2,b_1^{-1}b_2,4b_2)\\&+12b_2(10,2b_1,2b_1^{-1},6b_2)+6b_1(10,3b_1,b_1^{-1},2b_1^{-1}b_2,4b_2)+6b_1^{-1}(10,b_1,3b_1^{-1},2b_1b_2,4b_2)\\&+12b_1^{-1}(10,b_1,3b_1^{-1},3b_1b_2,b_1^{-1}b_2,2b_2)+12b_1(10,b_1^{-1},3b_1,b_1b_2,3b_1^{-1}b_2,2b_2)\\&+2b_1^{-1}(9,3b_1^{-1},3b_1b_2,3b_2)+2b_1(9,3b_1,3b_1^{-1}b_2,3b_2)+2(8,b_1,b_1^{-1},3b_1b_2,3b_1^{-1}b_2)\\&+18(11,2b_1,3b_1^{-1},b_1b_2,5b_2)+18(11,3b_1,2b_1^{-1},b_1^{-1}b_2,5b_2)+18b_2(9,b_1,2b_1^{-1},b_1b_2,5b_2)\\&+18b_2(9,2b_1,b_1^{-1},b_1^{-1}b_2,5b_2)+60(12,3b_1,3b_1^{-1},b_1b_2,b_1^{-1}b_2,4b_2)-132(13,4b_1,3b_1^{-1},b_1^{-1}b_2,5b_2)\\&-132(13,3b_1,4b_1^{-1},b_1b_2,5b_2)-34b_1^{-1}(11,b_1,4b_1^{-1},3b_1b_2,3b_2)-34b_1(11,4b_1,b_1^{-1},3b^{-1}b_2,3b_2)\\&-66b_2(10,2b_1,2b_1^{-1},6b_2)-52(12,3b_1,3b_1^{-1},6b_2)+246(14,4b_1,4b_1^{-1},6b_2)\end{aligned}$$
$$\begin{aligned}2F_{201}=&3(12,6b_1,b_1^2b_2,5b_2)+3b_1^{-2}(8,2b_1,b_1^2b_2,4b_1b_2,b_2)+12b_1^{-1}(10,4b_1,b_1^2b_2,2b_1b_2,3b_2)\\&+6b_1^{-1}(10,b_1^2,3b_1,3b_1b_2,3b_2)+12b_1^{-1}(10,4b_1,4b_1b_2,2b_2)+54(12,5b_1,b_1^2,b_1b_2,5b_2)\\&+30(12,6b_1,2b_1b_2,4b_2)-78(13,6b_1,b_1^2,6b_2)-38b_1^{-1}(11,5b_1,3b_1b_2,3b_2)\\&-150(13,7b_1,b_1b_2,5b_2)+146(14,8b_1,6b_2)\end{aligned}$$

cluster diagrams with nine u_2^{-1} lines. The work of Plischke and Chan[9] shows that there is no K_1 dependence in these orders, i.e., there are no six-point diagrams with seven u_2^{-1} (NNN) bonds and u_1 (NN) bonds, etc. Therefore, the contributions to eleventh and twelfth orders in u_2 which are not included in our L_1 through L_5 are just the above mentioned contributions from six-point diagrams with seven NNN bonds ($18u_2^{11}$), from the six-point diagram with six NNN bonds ($496u_2^{12}$) and from the seven-point diagrams with nine NNN bonds ($8u_2^{12}$). The twelfth-order low-temperature series

$$-\beta F=3K_2+\sum_m\left[\sum_n\frac{q_{mn}}{2}(u_1^{-n}+u_1^n)\right]u_2^m\ , \tag{3.8}$$

including the corrections to our high staggered field series are presented in Table VII.

IV. SERIES ANALYSIS

For a continuous transition the susceptibility related to order-parameter fluctuations diverges at the transition temperature K_c^{-1} as $(1-K/K_c)^{-\gamma}$; how-

TABLE VI. The coefficients $[n;rs]$ in $L_n(u_1,u_2)=\sum_{r,s}[n;r,s]u_1^r u_2^{3n-s}$ for the free-energy series in zero field (bcc lattice) Eq. (3.7).

	r	s	$2[n;rs]$		r	s	$2[n;rs]$
$n=1$	0	0	2.0	$n=5$	0	0	68 584.375
$n=2$	0	0	−15.0		0	1	−67 296.0
	0	1	6.0		0	2	34 536.0
	1	0	4.0		0	3	−9192.0
	−1	0	4.0		0	4	804.0
$n=3$	0	0	194 2/3		1	0	−45 680.0
	0	1	−120.0		−1	0	−45 680.0
	0	2	30.0		2	0	15 180.0
	1	0	−88.0		−2	0	15 180.0
	−1	0	−88.0		3	0	−2568.0
	2	0	12.0		−3	0	−2568.0
	−2	0	12.0		4	0	182.0
	−1	1	24.0		−4	0	182.0
	1	1	24.0		0	5	96.0
$n=4$	0	0	−3361.5		−1	1	35 856.0
	0	1	2706.0		1	1	35 856.0
	0	2	−1089.0		−1	2	−12 984.0
	0	3	166.0		1	2	−12 984.0
	1	0	1948.0		−1	3	1784.0
	−1	0	1948.0		1	3	1784.0
	2	0	−474.0		2	1	−7344.0
	−2	0	−474.0		−2	1	−7344.0
	3	0	44.0		2	2	1248.0
	−3	0	44.0		−2	2	1248.0
	0	4	6.0		2	3	8.0
	−1	1	−1056.0		−2	3	8.0
	1	1	−1056.0		3	1	528.0
	−1	2	216.0		−3	1	528.0
	1	2	216.0		−1	4	24.0
	2	1	108.0		1	4	24.0
	−2	1	108.0				

ever, for a discontinuous transition, the susceptibility does not have a divergent singularity at the transition temperature, although the smooth continuation of the high-temperature susceptibility may diverge at a lower temperature on a spinodal.

To locate the divergence of the high-temperature susceptibility for fixed values of $\alpha=K_1/K_2$, we have used standard Padé methods[11] to analyze the logarithmic derivative of the high-temperature series for the susceptibility appropriate to that value of α, i.e., χ_s for $K_1<1.5K_2$ and χ for $K_1>1.5K_2$. The apparent convergence of the series worsened as the values chosen for α neared 1.5, the mean-field "bicritical" point. This apparent convergence was improved somewhat by the use of a variable transformation which moved the competing singularity from $K_2=-K_{Ic}(\alpha)$, the critical point of the simple Ising antiferromagnet with the same value of the ratio $\alpha=K_1/K_2$ but both interactions negative, out to $-\infty$. The variable transformation used was $K_2'=\ln[1+K_2/K_{Ic}(\alpha)]$. This "second-order" phase boundary locating the divergence of the susceptibility at T_χ is shown in Fig. 2. As was found in Ref. 5, the index, γ, characterizing the divergence of the appropriate susceptibility is Ising-type ($\gamma\approx1.24$) for the whole range of K_1 agreeing with Landau theory for the ferromagnetic regime $K_1>1.5K_2$ but not for the AF_2 regime $K_1<1.5K_2$. This disagreement with the predictions of Landau theory has several explanations, only one of which is the fluctuation-induced first-order transition; it might also be due to the failure of short series to reflect the crossover from $n=1$ to $n=2$ type behavior.

To investigate the possibility of a fluctuation-induced first-order transition, we have determined

TABLE VII. Coefficients $q_{m,n}$ for the low-temperature expansion of the free-energy expansion in zero-staggered and external fields (bcc lattice) (3.8).

	n	$q_{m,n}$
$m=3$	0	+1.0
$m=5$	0	3.0
$m=6$	0	−7.5
	1	4.0
$m=7$	0	15.0
$m=8$	0	−57.0
	1	24.0
$m=9$	0	$180\frac{1}{3}$
	1	−88.0
	2	12.0
$m=10$	0	−496.5
	1	216.0
$m=11$	0	1773.0
	1	−1032.0
	2	108.0
$m=12$	0	−5771.75
	1	3732.0
	2	−446.0
	3	44.0

an estimate of the free-energy matching temperature, T_m, the transition temperature. Fixing K_1/K_2 and K_2, we have formed tables of Padé approximants $F(N,D,K_2,K_1/K_2)$ to the appropriate free-energy series in order to extrapolate our finite free-energy series to determine an estimate of $F(K_2,K_1/K_2)$.[6] For example, Table VIII presents the table of Padé approximants F_{AF_2} $(N,D,K_2=0.275,\ K_1/K_2=1.40)$ to the low-temperature free-energy series in the AF_2 phase, while Table IX presents the table of Padé approximants to the high-temperature free-energy series for the same values of K_2 and K_1/K_2. Graphing our estimates of the free energy in the paramagnetic phase, $F_P(K_2,K_1/K_2)$, and the free energy in the AF_2 phase, $F_{AF_2}(K_2,K_1/K_2)$ as a function of K_2 for fixed K_1/K_2 yields a graphical estimate of the matching temperature T_m, which is the transition temperature independent of whether the transition is first or second order. Figure 3 presents these free-energy graphs for $K_1/K_2=1.40$; the free energies have a physical intersection (where both free-energy slopes are positive, consistent with negative energies) at $K_2=T_m^{-1}=0.29$.

In addition to these graphical determinations of T_m, we have made more direct numerical determinations of T_m for fixed values of K_1/K_2 by equating the (N,D) Padé approximant of the high-temperature free-energy series to the (N',D') Padé

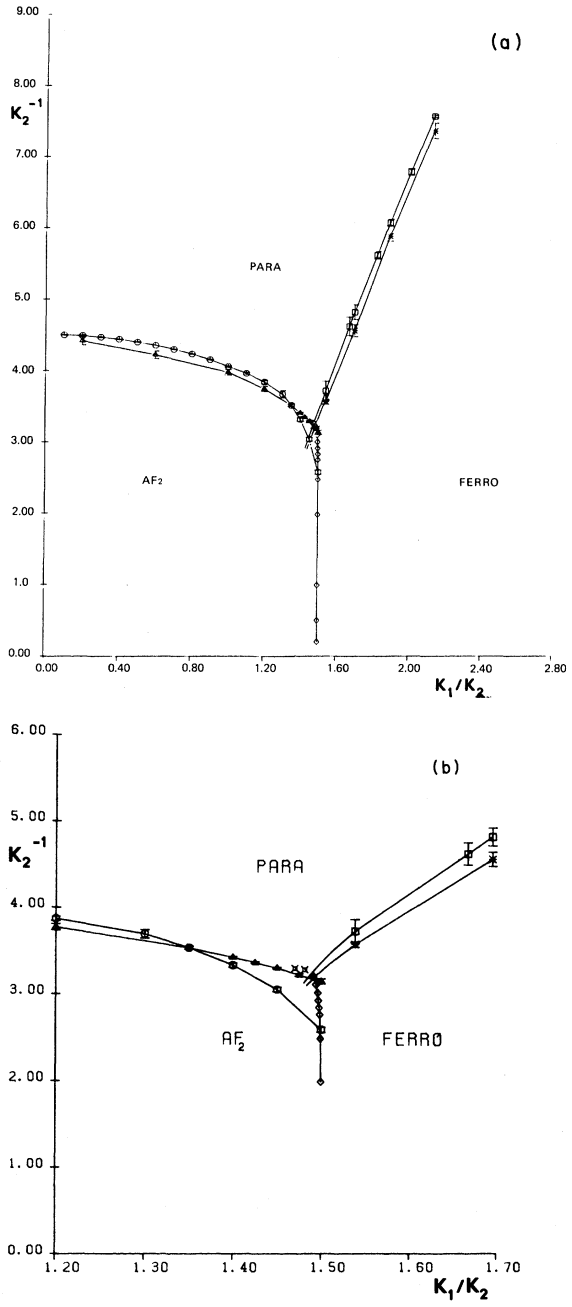

FIG. 2. The phase boundary of the bcc, spin-$\frac{1}{2}$ Ising model with competing interactions. The temperatures locating the divergence of the susceptibility, T_χ, are indicated by o for the staggered susceptibility and by □ for the susceptibility. The free-energy matching temperatures, T_m, are indicated by △ for the paramagnetic (PARA) to type two antiferromagnetic (AF_2) transition, by * for the PARA to ferromagnetic (FERRO) transition, and by ◇ for the AF_2 to FERRO transition. The ⊠ indicates the transition temperatures as determined by the Monte Carlo calculations of Ref. 4. (b) shows the region near the "bicritical point" in greater detail.

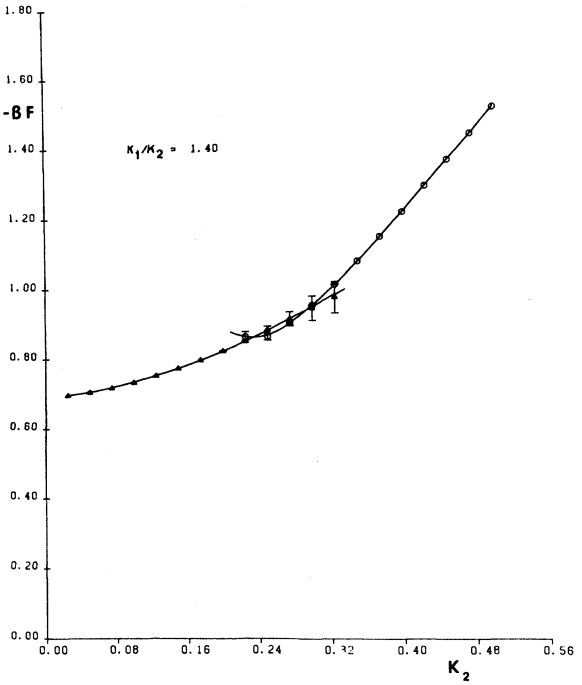

FIG. 3. The free-energy as a function of K_2, for $K_1/K_2=1.40$. The △ indicate our estimates from Padé approximants of the high-temperature, free-energy series, and the o indicate our estimates from Padé approximants of the low-temperature, free-energy series in the AF_2 phase.

approximant of the low-temperature, free-energy series; for the AF_2 phase,

$$F_P(N,D,K_2,K_1/K_2)=F_{AF_2}(N',D',K_2,K_1/K_2)\ . \tag{4.1}$$

Numerical solutions of this equation for K_2 provides a set of estimates of the location of the phase boundary, i.e., the value of K_2 on the phase boundary,

$$T_m^{-1}=K_2(N,D,N',D',K_1/K_2)\ .$$

Table X shows a subset of these estimates for $K_1/K_2=1.40$, and $(N',D')=(4,3),(4,4)$. In the usual way, we rely heavily on the near-diagonal, higher-order approximants to determine estimates of the "best value" of T_m and corresponding uncertainties which include most of the values from the near-diagonal, higher-order Padés. In Table XI and Fig. 2 we present these estimates of the matching temperature for the phase boundary between the paramagnetic and AF_2 phases, between the paramagnetic and ferromagnetic phases, and between the AF_2 and ferromagnetic phases. In the latter case, we determined the set of estimates locating the phase boundary by equating two Padé approximants to the free energies for fixed K_2

$$F_{AF_2}(N,D,K_2,K_1/K_2)=F_{\text{ferro}}(N',D',K_2,K_1/K_2) \tag{4.2}$$

and then solving numerically for the value of K_1/K_2 on the phase boundary.

V. CONCLUSIONS

The results of our analysis are most clearly summarized in Fig. 2. In the near AF_2 regime, i.e., $K_1 \lesssim 1.5K_2$, our estimate of the transition temperature from free-energy matching, T_m, is as much as 15% larger than T_χ, the temperature locating the divergence of the staggered susceptibility, which supports the conclusions of Ref. 4 that the transition in the near AF_2 regime is first order.

Elsewhere, our estimate of T_m is a few percent below T_χ. Experience has shown that these methods of determining T_m consistently underestimate the transition temperature by about 5% or less.[6] This tendency to underestimate T_m is reflected in our results for the ferromagnetic regime where T_χ should equal T_m since the transition is certainly

TABLE VIII. $[N,D]$ Padé approximants to the low-temperature energy for the AF_2 ground state at $K_1/K_2=+1.40$ and for $K_2=0.275$. We estimate $F_{AF_2}(0.275,1.40)=0.898\pm0.008$.

N \ D	1	2	3	4	5	6	7
1		0.909 364	0.886 352	0.899 924	0.902 838	0.891 963	0.903 162
2	0.871 608	0.891 024	0.892 681	0.903 305	0.900 404	0.896 625	
3	0.884 249	0.893 034	0.889 835	0.896 311	0.897 380		
4	0.883 996	0.907 107	0.898 483	0.897 879			
5	0.889 650	0.895 765	0.897 781				
6	0.888 946	0.899 859					
7	0.893 428						

TABLE IX. $[N,D]$ Padé approximants to the high-temperature free-energy for the AF_2-ground state at $K_1/K_2=1.40$ and for $K_2=-0.275$. We estimate $F_P(0.275,1.40)=0.91\pm0.04$.

N \ D	1	2	3	4	5	6	7	8	9
1		0.9189	0.8881	0.9330	0.8641	0.9835	0.7586	1.2267	0.1823
2	0.9429	0.9007	0.9070	0.9051	0.9086	0.9045	0.9119	0.9012	
3	0.8580	0.9086	0.9055	0.9064	0.9066	0.9072	0.9074		
4	1.3743	0.9039	0.9068	0.9067	0.9063	0.9074			
5	0.7708	0.9117	0.9066	0.9068	0.9076				
6	0.6364	0.8986	0.9075	0.9074					
7	0.7078	0.9299	0.9073						
8	0.6877	0.8706							
9	0.6949								

second order. Furthermore, this tendency to underestimate T_m supports the slightly higher values of the Monte Carlo determination of the transition temperatures in the near AF_2 regime, and further strengthens the conclusion that the transition is first order in this regime. The agreement of the three complementary approaches, ϵ expansion and Monte Carlo of Ref. 4, and this series work lends additional credence to our mutual conclusion about the near AF_2 regime.

Further into the AF_2 regime, $K_1/K_2<1.3$, our estimate of T_m is a few percent below T_χ, suggesting that $T_m\approx T_\chi$ indicative of a second-order transition. Although our results do not rule out a first-order transition, they do show that any first-order transition would be nearly second order, in that the staggered susceptibility would be nearly divergent, order-parameter discontinuities would be small, etc., over a large range of values of K_1. If the transition is second-order, our failure to observe XY-like indices in the deep AF_2 regime is undoubtedly due to the failure of our short (ten term) series to reflect the crossover from the $K_1=0$ Ising-like behavior to the finite K_1 XY-like behavior because the crossover is characterized by a crossover exponent which is expected to be small.[7,12] Near this $K_1=0$ decoupling critical point, recent work has shown that while the pairwise interaction K_1 is irrelevant, in second order, it generates a relevant ferromagnetic, four-spin interaction with crossover exponent $\phi=\alpha_I\simeq0.12$.[12] Past experience with such ferromagnetic four-spin couplings in other systems leads one to expect crossover from the decoupling critical point to a first-order transition.[13] If the transition in this system is also first order, the scaling form for the free energy from Ref. 12 leads to the conclusion that the latent heat varies as $L\propto K_1^{2(\alpha_I^{-1}-1)}$; the large power of K_1, $2(\alpha_I^{-1}-1)\simeq15$, would imply a "nearly second-order" transition with small discontinuities, etc., in the deep AF_2 regime. Unfortunately, our work is not able to distinguish between this more likely possibility, a first-order transition with small discontinuities, and the possibility of a second-order transi-

TABLE X. Location of phase boundary for $K_1/K_2=1.40$ from matching $F_P(N,D,K_2,1.40)$ with $F_{AF_2}(N',D',K_2,1.40)$ to determine $K_2(N,D,N',D',1.40)$.

N \ D	3	4	5	6	7
		$K_2(N,D,4,3,1.40)$			
3	0.2867	0.2890	0.2887	0.2905	0.2904
4	0.2883	0.2887	0.2890	0.2904	
5	0.2887	0.2882	0.2916		
6	0.2898	0.2908			
7	0.2904				
		$K_2(N,D,4,4,1.40)$			
3	0.2872	0.2895	0.2892	0.2909	0.2909
4	0.2888	0.2892	0.2895	0.2909	
5	0.2892	0.2886	0.2920		
6	0.2903	0.2912			
7	0.2908				

TABLE XI. Estimates of the phase boundary location from free-energy matching.

Paramagnetic-AF_2 boundary		Paramagnetic-ferromagnetic boundary		AF_2-ferromagnetic boundary	
K_1/K_2	K_2	K_1/K_2	K_2	K_1/K_2	K_2
1.500	0.316±0.006	1.5385	0.278±0.005	1.488±0.020	0.30
1.475	0.309±0.003	1.6950	0.217±0.008	1.491±0.008	0.31
1.450	0.3015±0.0020	1.8868	0.168±0.004	1.494±0.004	0.32
1.425	0.296±0.002	2.1277	0.134±0.004	1.496±0.003	0.33
1.400	0.291±0.003			1.4970±0.0015	0.34
1.350	0.282±0.003			1.4978±0.0010	0.35
1.200	0.265±0.005			1.4984±0.0004	0.36
1.000	0.250±0.005			1.4993±0.0001	0.40
0.600	0.236±0.006				
0.200	0.226±0.006				

tion with Ising-type effective exponents due to the smallness of the crossover exponent.

ACKNOWLEDGMENTS

We are grateful to D. Jasnow for suggesting this problem and for many helpful discussions. We are grateful to David Huse for making us aware of his work and its impact on our own. We also wish to thank R. B. Griffiths and D. P. Landau for helpful discussions. The authors gratefully acknowledge research support through NSF-EPSCoR Grant No. ISP 8011453-18.

[1]O. G. Mouritsen, S. J. Knak Jensen, and Per Bak, Phys. Rev. Lett. 39, 629 (1977); S. A. Brazovsky, I. E. Dzyaloshinsky, Zh. Eksp. Teor. Fiz. Pis'ma Red. 21, 360 (1975) [JETP Lett. 21, 164 (1975)].

[2]J. S. Smart, *Effective Field Theories of Magnetism* (Saunders, Philadelphia, 1966).

[3]D. Mukamel and S. Krinsky, Phys. Rev. B 13, 5065 (1976).

[4]J. Banavar, D. Jasnow, and D. P. Landau, Phys. Rev. B 20, 3820 (1979).

[5]M. Plischke and J. Oitmaa, Phys. Rev. B 19, 487 (1979).

[6]D. Saul, M. Wortis, and D. Stauffer, Phys. Rev. B 9, 4964 (1974).

[7]Reference 4 states that evidence supports a crossover exponent less than 1. It seems likely that this exponent is on the order of α_I on the basis of simple scaling arguments and naive series analysis.

[8]M. Ferer, M. A. Moore, and M. Wortis, Phys. Rev. B 4, 3954 (1971).

[9]M. Plischke and C. F. S. Chan, Can. J. Phys. 54, 1646 (1976).

[10]C. Domb, in *Phase Transitions and Critical Phenomena,* edited by C. Domb and M. S. Green (Academic, New York, 1974), Vol. 3, p. 357; M. F. Sykes, J. W. Essam, and D. S. Gaunt, J. Math. Phys. 6, 283 (1965).

[11]D. S. Gaunt and A. S. Guttmann, in *Phase Transitions and Critical Phenomena,* edited by C. Domb and M. S. Green (Academic, New York, 1974), Vol. 3, p. 181.

[12]David A. Huse and Michael Fisher, J. Phys. C 15, L585 (1982).

[13]A. Aharony, *Phase Transitions and Critical Phenomena,* edited by C. Domb and M. S. Green (Academic, New York, 1976) Vol. 6; R. V. Ditzian, J. R. Banavar, G. S. Grest and L. P. Kadanoff, Phys. Rev. B 22, 2542 (1980).